A Bayesian implementation of Quality-by-Design for the development of Cationic Nano-Lipid for siRNA Transfection

Thierry Bastogne, Lucie Hassler, Jonathan Bruniaux, Magalie Thomassin, Xavier Gidrol, Eric Sulpice and Fabrice P. Navarro

***Abstract*—Unlike Quality by Testing approach, where products were tested only after drug manufacturing, Quality by Design (QbD) is a proactive control quality paradigm, which handles risks from the early development steps. In QbD, regression models built from experimental data are used to predict a risk mapping called *Design Space* in which the developers can identify values of critical input factors leading to acceptable probabilities to meet the efficacy and safety specifications for the expected product. These empirical models are often limited to quantitative responses. Moreover, in practice the smallness and incompleteness of datasets degrade the quality of predictions. In this study, a Bayesian approach including variable selection, parameter estimation and model quality assessment is proposed and assessed using a real case study devoted to the development of a Cationic Nano-Lipid Structures for siRNA Transfection. Two original model structures are also included to describe both binary and percentage response variables. The results confirm the practical relevance and applicability of the Bayesian implementation of the QbD analysis.**

***Index Terms*—Statistics, Bayes, Quality by Design, Nanomedicine, siRNA.**

T. Bastogne is with CRAN, Université de Lorraine and INRIA BIGS, Nancy, France (e-mail: thierry.bastogne@univ-lorraine.fr).

L. Hassler is with CYBERNANO, Nancy, France.

J. Bruniaux is with Univ. Grenoble Alpes, F-38000 Grenoble, France and CEA, LETI, MINATEC Campus, Division for biology and healthcare technologies, F-38054 Grenoble, France.

M. Thomassin is with CRAN, Université de Lorraine, Nancy, France

X. Gidrol is with Univ. Grenoble Alpes, F-38000 Grenoble, France and CEA, IRIG, Biomics lab, F-38054 Grenoble, France.

E. Sulpice is with Univ. Grenoble Alpes, F-38000 Grenoble, France and CEA, IRIG, Biomics lab, F-38054 Grenoble, France.

F. P. Navarro is with CEA LETI, Grenoble, France and CEA, LETI, MINATEC Campus, Division for biology and healthcare technologies, F-38054 Grenoble, France.

I. Introduction

Due to their complex structure, the development of non-biological complex drugs must comply with the set of ICH[1] Q8-Q11 guidelines to better control quality and safety as early as first steps of development. One holistic approach to today's current challenges within the nano-pharmaceutical industry is to focus on the Pharmaceutical Quality by Design (QbD), which begins with predefined objectives and emphasizes product and process understanding, based on data-driven modeling and quality risk assessment [1], [2].

Since 2017, QbD has become more and more popular in the nanomedicine community to better control quality and safety during the synthesis and production phases [3], [2]. Nevertheless, some important deficiencies and inadequacies have also been identified in these

[1]International Conference on Harmonization

QbD implementations [4]. One of them concerns the computation of the Design Space, a multidimensional diagram of probabilities, which measures the likelihood of satisfying quantitative requirements on output variables. These probabilities are estimated from mathematical models describing the relationships between the input-output variables. When mechanistic models are not available, we use empirical models. To identify them, experimental datasets must be compiled and the most popular technique is to apply design of experiments (DoE). This statistical approach to the preparation of the experimental setup makes it possible to reduce the number of trials to obtain an acceptable accuracy on the model predictions. Nevertheless, in biology, it often happens that certain experiments fail and, unfortunately, the conditioning of the estimation problem is very sensitive to the loss of experience within the learning dataset. The direct consequence is an imprecise model and the final result is either an underestimation or an overestimation of the risks not to comply with the quality/safety requirements.

Since the QbD approach relies on successive investigation cycles, the knowledge from the previous round can be partially reused in the current stage through a Bayesian modeling approach. This explains why these methods have often been used in QbD studies [5][6][7][8]. Nevertheless, several hurdles still need to be crossed over to improve their applicability to QbD studies. Two specific issues are addressed in this study: the analysis of qualitative responses and missing data. To illustrate the applicability of the proposed solution, we present a study case based on the development of lipid nanoparticles for siRNA transfection in which the two examined critical quality attributes are their stability and the transfection efficiency. The initial experimental setup was based on a mixture design of experiments and was composed of 36 different trials. Unfortunately, some of those experimental conditions led to unstable nanoparticles, which finally cut in half the number of nanoparticles to be used during the transfection efficiency tests. In that situation, the Bayesian regression paradigm can be used to handle the ill-conditioning of the estimation problem by introducing prior knowledge. The methodological contribution covers both the variable selection, parameter estimation and model validation. Moreover, to address the issues related to the qualitative response modeling and to account for the constraints on the possible values taken by a percentage response, a Bayesian estimation procedure is applied to a logistic model.

II. Material and methods

A. Quality-by-Design compounds

Quality by design (QbD) is an holistic, proactive and integrative approach to drug development that begins with predefined objectives and emphasizes product and process understanding, based on sound science and quality risk management [9]. The overarching goal of QbD is to improve biological therapeutics safety and efficacy, while additional benefits include the reduction of cost and the potential for faster regulatory approval of new drugs. This approach can be broken down into two main parts. The first is rather statistical and aims to assess risks and identify the normal operating region. The second is technological and consists of integrating sensors, probes, control units and database management systems to better control the manufacturing process and achieve quality goals in a sustainable way. The statistical part of the QbD approach is composed of four main steps as presented in Figure1: (i) the product profiling, (ii) the experimental phase, (iii) the data analysis and (iv) the knowledge extraction.

1) Quality Target Product Profile: The first step of QbD is to define the Quality Target Product Profile (QTPP) of the ideal drug product we wish to develop.

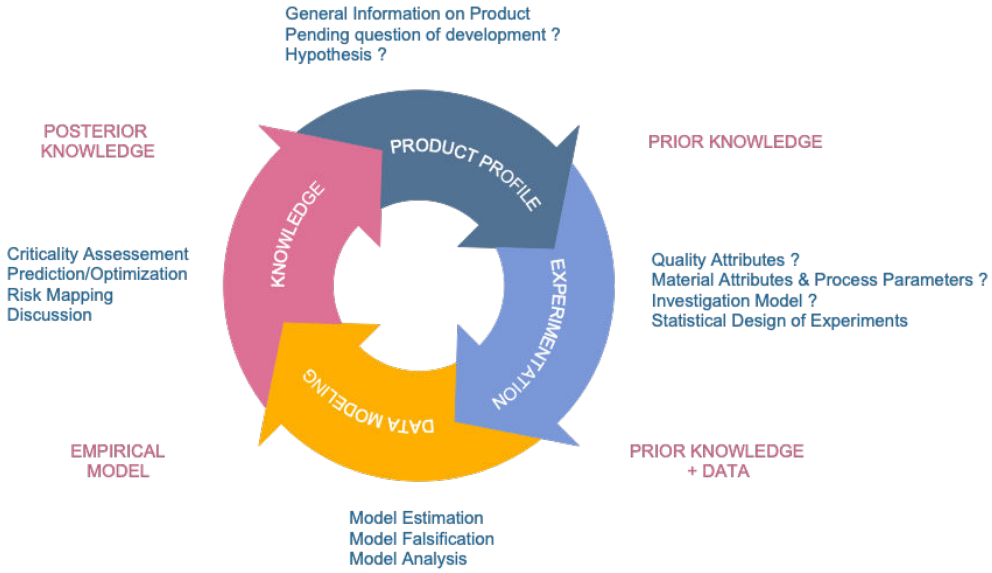

Fig. 1. Quality-by-Design cycle of drug development decomposed into four steps. The procedure is re-executed at each critical development question.

This includes information like the intended use, dosage form & appearance, route of administration, stability, physical attributes, purity, sterility and water content, but it can also include business information about the targeted market, as emphasized in [10]. Its content must be regularly updated throughout the development process. As nothing new is discussed on this point herein it is not detailed in this article.

2) CQA Definition and specification: The experimentation phase of the QbD cycle starts by defining the output and input variables. A critical quality attribute (CQA) is a physical, chemical or biological property or any other characteristics, which that must be kept within an appropriate range to ensure the desired product quality defined in the QTTP. CQA can be regarded as output variables associated with efficacy/safety or quality objectives. Critical manufacturing attributes (CMA) belong to the first category of input factors able to cause variability of CQA. They are associated with the formulation parameters of the nanoproduct. Critical process parameters (CPP) are the second category of input variables. They are related to the manufacturing parameters. The experimentation phase also includes (i) the design of experiments to stimulate in a minimum of tests CPP and CMA and (ii) the collection of measurements on the CQA during the experiments. The experimental data thus collected will allow the next step to better understand the cause-effect relationship between those variables to finally predict the risks of not complying the efficacy/safety/quality specifications.

3) Data-driven modeling: The mathematical relationship between quality outcomes (CQA) and input factors (CMA and CPP) is experimentally determined in a third step using specific data-driven modeling methods. In practice, response surface equations, a class of polynomial models, are often used to describe the links between input and output variables. This type of model enables in QbD to compute a Design Space: a risk mapping tool used to identify the operating region of quality.

4) Knowledge extraction and risk prediction: The Design Space is a graphical representation used to determine the CPP values allowing the quality requirements to be met with a controlled probability. The graph can be divided into four regions of probability:

- the Out Of Specification (OOS) region, in which the probabilities of meeting the technical requirements on CQA are too small. In such a situation, deeper investigations are required to understand the reasons for unacceptance;
- the Proven Acceptance Region (PAR) , in which the probabilities of meeting the technical requirements are acceptable but some adjustments should be made to access the NOR;
- the Normal Operating Region (NOR) corresponds to the desired region where CQA have a high degree of probability of complying with their quality specifications;
- the Control Operating Region (COR) is a subspace of NOR in which an automated control system has to maintain the operating point.

In this study, we focus on the last three stages of the cycle. Since the 19th century, the scientific investigation has been essentially inspired by an approach integrating deductive and inductive methods, in which the today's prior is updated by new data to become a posterior knowledge that will serve as tomorrow's prior, and so forth. The Bayesian inference [11] engine as well as the Quality by Design paradigm work namely the same way, as illustrated in Figure 1. This is one of the reasons that motivated us to integrate the two approaches.

B. Physico-chemical characterization & Biological assays

All aspects of the material characterization, cell culture conditions, stability testing, cytotoxicity assays, inhibition studies, internalisation estimation, co-localization quantification and transfection efficacy are detailed in appendices of this document.

C. Definition of critical quality and material attributes

1) CQA Definition: Two quality attributes were identified as critical in this study.

- Y_s is a critical safety attribute related to the LNP stability. This output variable takes only two values: $\{0; 1\}$ to describe unstable and stable states respectively.
- Y_e is a critical efficacy attribute related to the siRNA transfection rate. Specification on Y_e: a minimun of 30% of efficacy is expected. The transfection efficiency is in fact a downregulation efficiency based on the monitoring of the extinction of GFP expression.

2) CMA Definition: Four material attributes were tested to identify their potential effects on the two CQA previously defined:

- X_1 is the DOTAP proportion (%) in the LNP content;
- X_2 is the concentration of PEG surfactant (%);
- X_3 is the Lecithin proportion (%);
- X_4 is the LNP size (small, medium, large).

D. Statistical Analysis

1) Design of Experiments: A D-optimal mixture design was implemented to select 36 formulations to be synthesized and tested in *in vitro* assays. This design was computed with the Design Expert Software. The composition of those 36 LNPs is presented in Table I. 13 LNPs did not comply with polydispersity specifications and were eliminated at the beginning of the study. As a consequence, only 23 LNPs were used in the stability analysis. Finally, having removed the unstable LNPs, there remained only 15 candidates to test the transfection

efficiency. Because of those missing data, the estimation of the response surface model parameters becomes ill-conditioned. A Bayesian estimation strategy can be a solution to overcome that issue and regularize the estimation problem. In the best case, prior data collected during pilot experiments can be used to estimate the prior distributions of some parameters. Otherwise, a weakly informative default prior is designed to provide moderate regularization and to improve the computation stabilization. That option was used in this study.

2) Bayesian Estimation Method: The bayesian inference techniques are more and more used in Pharmacology [12] and now recommended by FDA in numerous studies such as medical device clinical trials [13], clinical trials to evaluate the safety of human drugs or biological products [14] as well as biomarker qualification [15]. Data-driven Bayesian modeling methods are particularly relevant when biological datasets are small as is often the case with the use of statistical methods to design experiments. In this context, the classical tests and regression techniques based on the frequentist paradigm are often biased and too optimistic. In QbD studies, a large majority of design spaces, computed and presented in most of the scientific publications, rely on average responses and do not account for the prediction uncertainty [16], [17], [18], [19], [20], [21], [22], [23], [24], [25], [26], [27]. The Bayesian estimation methods bring a natural framework to efficiently handle this problem [28], [29].

The idea behind the Bayesian framework is quite simple. From observed data $y = (y_1, ..., y_n)$, n realizations of a variable Y whose distribution depends on both a parameter vector θ and explanatory variables $X = (x_1, ..., x_d)$, we try to estimate θ considering it as a random variable. The probability distribution of θ is unknown and has to be determined. To that aim, we first need to specify a *prior* distribution based on previous knowledge about the parameter and then update this information by using the new data we have in possession owing to the following Bayes formula:

$$p(\theta \mid y, x) \quad \propto \quad p(y \mid \theta, x) \cdot p(\theta) \tag{1}$$

where $p(\theta \mid y, x)$ denotes the *posterior* distribution of θ given observed data y and the values x of the input factors X, which have been previously fixed by a design of experiments. $p(y \mid \theta, x)$ and $p(\theta)$ are the likelihood function and *prior* distribution on θ respectively. The

	x_1	x_2	x_3	x_4		Y_s	Y_e
Run	DOTAP	PEG	Lecithine	Size target	PDI	Stable	Transfection PC3-GFP
1	0.2	0.2	0.4	3	0.223	NA	
2	0.53	0.21	0.06	2	0.377	NA	
3	0.52	0.22	0.06	1	**0.16**		70.94
4	0.46	0.48	0.06	1	0.366	NA	
5	0.54	0.21	0.06	3	0.315	NA	
6	0.41	0.29	0.26	3	**0.172**	no	
7	0.2	0.2	0.4	2	**0.184**	no	
8	0.21	0.53	0.06	3	**0.187**		18.15
9	0.21	0.53	0.06	2	**0.161**		12.1
10	0.27	0.23	0.5	3	**0.162**	no	
11	0.47	0.47	0.06	2	**0.147**		28.72
12	0.2	0.65	0.15	2	**0.175**		20.75
13	0.47	0.47	0.06	3	0.222	NA	
14	0.2	0.45	0.35	2	**0.15**		13.52
15	0.7	0.2	0.1	2	**0.163**	no	
16	0.47	0.47	0.06	2	**0.148**		44.35
17	0.21	0.53	0.06	2	**0.181**		19.7
18	0.2	0.65	0.15	1	0.258	NA	
19	0.7	0.2	0.1	3	0.304	NA	
20	0.27	0.23	0.5	2	**0.135**	no	
21	0.27	0.23	0.5	1	0.381	NA	
22	0.2	0.2	0.4	1	0.249	NA	
23	0.48	0.2	0.29	1	0.274	NA	
24	0.21	0.53	0.06	1	0.458	NA	
25	0.7	0.2	0.1	2	**0.167**	no	
26	0.2	0.43	0.32	1	0.327	NA	
27	0.47	0.2	0.29	2	**0.155**	no	
28	0.53	0.21	0.06	2	0.234	NA	
29	0.2	0.65	0.15	3	**0.198**		5.77
30	0.27	0.23	0.5	2	**0.129**	no	
31	0.7	0.2	0.1	1	**0.192**		31.27
32	0.54	0.29	0.17	1	**0.187**		45.73
33	0.54	0.29	0.07	1	**0.192**		68.11
34	0.27	0.65	0.08	2	**0.184**		7.19
35	0.4	0.48	0.12	2	**0.154**		17.09
36	0.4	0.48	0.07	2	**0.19**		28.79

TABLE I

LIST OF THE 36 EXPERIMENTAL CONDITIONS BASED ON A D-OPTIMAL MIXTURE DESIGN. MODALITIES $1, 2, 3$ OF x_4 STAND FOR SMALL: (1), MEDIUM: (2) AND LARGE: (3) TARGETED DIAMETERS. NA INDICATES THAT STABILITY WAS NOT TESTED SINCE THE PDI CONDITION WAS NOT MET. PDI VALUES IN BOLD INDICATE THOSE MEETING THE DESIRED SPECIFICATION (PDI$<$0.2)

posterior distribution contains updated information about the parameter after observing the data y [11].

In most cases, we cannot obtain the exact and explicit form of the *posterior* distribution and the best we can do is to get a sample from it by using numerical methods such as MCMC algorithms [30] or the ABC method [31]. Once the posterior distribution $p(\theta|y,x)$ estimated, we have to calculate the *posterior* predictive distribution in order to build the design space. This distribution allows us to digitally replicate data $\tilde{y}$ from the *posterior* distribution of the parameters. It is possible to compute $\tilde{y}$ either from the original values x or from new values $\tilde{x}$ of X. Both distributions $p(.|y,x)$ and $p(.|y,x,\tilde{x})$ are defined respectively by the two following equations:

$$p(\tilde{y}|y,x) = \int_{\Theta} p(\tilde{y}|\theta,x)p(\theta|y,x)d\theta, \tag{2}$$

$$p(\tilde{y}|y,x,\tilde{x}) = \int_{\Theta} p(\tilde{y}|\theta,\tilde{x})p(\theta|y,x)d\theta. \tag{3}$$

Let $\tilde{Y}|_{y,x,\tilde{x}}$ be the variable whose distribution is the *posterior* predictive distribution defined in (3). Thanks to this variable, the normal operating region within the design space is then defined as follows:

$$\begin{aligned} NOR &= \left\{ \tilde{x} \ ; \ \mathbb{P}(\tilde{Y}|_{y,x,\tilde{x}} \in \Lambda \ ) \geq \rho \right\} \\ &= \left\{ \tilde{x} \ ; \ \int_{\Lambda} p(\tilde{y}|y,x,\tilde{x})d\tilde{y} \ \geq \rho \right\} \end{aligned} \tag{4}$$

where $\mathbb{P}(\cdot)$ is a probability function, $\tilde{x}$ is a vector of values taken by the critical material attributes and/or critical process parameters. $\{\tilde{x}\}$ denotes the predicted NOR subspace, *i.e.* a subset of CMA/CPP values for which we have a probability greater than ρ to meet the expected specifications Λ on the predicted CQA: $\tilde{Y}$. The other regions: PAR and OOS are defined by the same equation but with different values of ρ.

The identification of the design space requires to determine the cause-effect relationship between Y and X. In practice, this relationship is often described by a response surface model identified from experimental datasets (y and x) collected after the application of a specific design of experiments [32], [33]. Unknown parameters of the response surface model are gathered in the vector θ. The structure of the response surface model is defined in sections II-D3 and II-D5 for the two CQA. In this study, a Bayesian approach is proposed to address several key issues before computing the design space.

a) **Variable Selection.** The first step is to choose the model structure that best fits the data. This step includes the selection of the most informative critical material attributes. The Bayes Factor is used to that aim [34].

b) **Parameter Estimation.** The second step is devoted to the model parameter estimation from experimental data.

c) **Model Evaluation.** Before using this empirical model to compute the design space, its ability to fit and predict the two CQA behaviors in the experimental domain has to be tested. The posterior predictive checking and the leave-one-out cross-validation techniques are employed for this purpose.

d) **Design Space Determination.** The NOR, PAR and OOS regions of the design space are then determined by calculating with equation (3) which proportions of the predicted CQA values meet the quality requirements.

3) Response surface modeling of the LNP stability: the first CQA examined in this study is noted Y_s and deals with the LNP stability. Since this CQA is binary, a logistic regression model was used herein. This technique is a generalization of the linear regression model where Y_s is described by a Bernoulli variable:

$$Y_{s,i} = Ber(\pi_{s,i}), \ i = 1, ..., 36 \tag{5}$$

where i denotes the i-th experimental condition of the design and $\pi_{s,i}$ is the parameter to be estimated, which should always be contained in the interval $[0, 1]$. To account for this constraint, we apply a transformation using the *logit* (noted g) function defined as follows:

$$g : [0, 1] \to \mathbb{R} \tag{6}$$

$$\pi \mapsto \log(\frac{\pi}{1-\pi}) \tag{7}$$

and thus :

$$g^{-1} : \mathbb{R} \to [0, 1]$$

$$z \mapsto \frac{e^z}{1+e^z}. \tag{8}$$

The model used for the LNP stability is described by the following equation:

$$\pi_{s,i} = g^{-1}(x_{i\bullet}b) = \frac{e^{b_0+\sum_{j=1}^{4} b_j x_{i,j}}}{1+e^{b_0+\sum_{j=1}^{4} b_j x_{i,j}}}. \tag{9}$$

where $x_{i\bullet}$ is the i-th row of the DoE matrix x, defined in Table I, and $x_{i,j}$ denotes the (i, j) entry of x. $j = \{1, 2, 3, 4\}$ is the CMA index.

4) Prior Modeling for the Stability Model: as we had no accurate *prior* knowledge on each parameter, a weakly informative default *prior* was chosen. These priors are designed to provide moderate regularization and to improve the computation stabilization. The way **rstanarm** attempts to make priors weakly informative by default is to internally adjust the scales of the priors, considering the data. First, all *prior* are set to a specific value. For the logistic regression, Gelman and al. (2008) recommend to use a Cauchy distribution with center 0 and scale 2.5, and a scale of 10 for the intercept [35]. Then, by considering the data we have, the priors on parameters were adjusted as follows: the β_0 scale is multiplied by $sd(y)$: the empirical standard deviation computed on the measured values of the response variable Y_s. The scales of the other model parameters are divided by $sd(x_j)$, where $sd(x_j)$ denotes the standard deviation computed on values of the input factor x_j associated with the corresponding parameter β_j. In addition, we assumed *prior* independence of the coefficients.

5) Response Surface Modeling of the Transfection Efficiency: the random variable Y_e denotes the percentage of siRNA transfection. This efficiency attribute is also described by a logistic model:

$$\log\left(\frac{Y_{e,i}}{1-Y_{e,i}}\right) = b_0 + \sum_{j=1}^{4} b_j x_{i,j} + E_i \tag{10}$$

where $E_i \overset{\text{iid}}{\sim} \mathcal{N}(0, s^2)$.

6) Prior Modeling for the Transfection Model: prior modeling for the transfection model is quite the same as for the stability model in section II-D4, we also use weakly informative *priors*. Cauchy distribution with center 0 and scale 2.5 is allocated for the β parameters, except for the intercept, which follows a Cauchy distribution with center 0 and scale 10. Then, the *prior* scales have to be adjusted considering the data, in the same way as it was explained for the stability model.

7) Variable selection with the Bayes Factor: at the origin, the Bayes Factor (BF) is a criterion used to compare the plausibility of two models but its principle was adapted to the variable selection in regression applications [36]. For each regressor, a test is applied by comparing the complete model, composed of all the explanatory variables, with the one without the j-th regressor. More precisely, the BF criterion for the j-th regression variable x_j is defined as the ratio of two marginal posterior likelihoods associated with the two competing models :

$$BF_j = \frac{L(y|\mathcal{M})}{L(y|\mathcal{M}_{-j})} \tag{11}$$

where $L(y|\mathcal{M}) = \int l(y|\mathcal{M}, \theta)p(\theta|\mathcal{M})d\theta$ is the likelihood function of the observed data y, given the model $\mathcal{M}$ whose parameters follow the posterior distribution: $p(\theta|\mathcal{M})$. This also applies to $\mathcal{M}_{-j}$ and θ_{-j} for

$L(y|\mathcal{M}_{-j})$. A higher value of BF_j means a higher level of the explanatory power for x_j.

8) Model evaluation with the PPC: the posterior predictive check (PPC) is a Bayesian technique to assess the appropriateness of the model to fit the data [37]. Its principle is to build up replicate datasets y^{rep} to be compared with real data through histograms or dedicated statistics of information. In this study, PPC was implemented with 4000 replicates.

a) Stability Response: however, PPC is not suited to characterize binary responses. Instead of using histograms, we propose an original diagram composed of 10 black and white bars. Each bar is decomposed into 25 segments corresponding each to the stability response after each assay. The first bar is the reference composed of the measured responses to be compared with the remaining bars associated with the simulation replicates. To illustrate the results coming from the 4000 replicates, we also built an average confusion matrix to estimate the mean sensitivity and specificity criteria.

b) Efficiency Response: for quantitative responses such as the percentage of efficiency, a quantity entitled *ppp-value* may be associated with the PPC test. The *ppp-value* corresponds to the probability for the replicate data to be greater than the observations. A targeted value for *ppp-value* is to be equal to 0.5.

9) Model evaluation with the LOO-CV: the Leave-One-Out Cross-Validation (LOO-CV) method aims at assessing the ability of the model to provide accurate predictions [38]. Its principle consists in dividing the observed dataset into n samples where n is the number of data points. Each sample is a *train set* in which the i-th observation is missing. It is used to fit the model and to test its ability to predict the remaining observation. The predictive feature of a model has to be checked before using it to build a relevant Design Space. A statistics, noted p_{LOO} thereafter, is used to compute the estimated effective number of parameters. If the model is well specified, p_{LOO} is expected to be smaller than or similar to the total number of parameters in the model.

III. Results

A. Estimation results for the stability model

TABLE II
BF values for the stability response (Savage-Dickey density ratio)

Variable	BF
X_1	0.7
X_2	3.88
X_3	1.39
X_4	23.94

1) Model Selection: values of the BF statistics given in Table II show that X_4 (LNP size) is the most critical material attribute on stability, far ahead of X_2 (PEG proportion). Only those two variables have been kept to explain the stability response thereafter.

2) Parameter Estimation: after the variable selection, the reduced model structure is given by :

$$\pi_{s,i} = g^{-1}(x_i b) = \frac{e^{b_0+b_2x_{2,i}+b_4x_{4,i}}}{1+e^{b_0+b_2x_{2,i}+b_4x_{4,i}}}. \qquad (12)$$

The estimated values of the model parameters, provided by the MCMC technique, are given in Table III. Figure 2 shows the posterior distributions associated with the three parameters of the stability logistic model defined in (12). Signs of the two coefficients show that the probability of stability is increasing with x_2 (PEG proportion) but decreasing with the rising of x_4 (LNP size). This model is used thereafter to predict the LNP stability for other pairs of values for X_2 and X_4.

3) Model evaluation: the posterior predictive check was applied to (12) to assess its appropriateness to fit the data. Its principle is to compare histograms of replicated data (y^{rep}) with the one of the measured data. However,

TABLE III

ESTIMATED VALUES, STANDARD DEVIATIONS, AND MAIN QUANTILES FOR THE LOGISTIC MODEL PARAMETERS

Parameter	Mean	SD	10%	50%	90%
b_0	4.1	8.9	-4	3	13.2
b_2	57.0	49.2	19.1	42.0	107.8
b_4	-177.9	155.0	-335.0	-132.6	-59.6

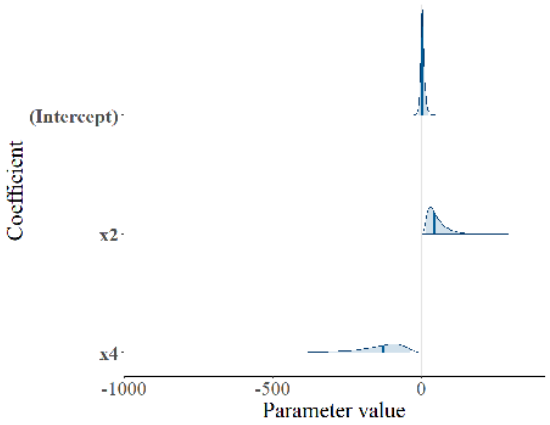

Fig. 2. Posterior distribution of the three parameters that compose the stability logistic model

this description is not suited to our binary response. In Figure 3, we propose an original diagram composed of black and white bars, the first one represents observed data and others correspond to predictions (here we show only 10 bars on the 4000 replications that have been performed). Each bar is decomposed into 25 segments corresponding to the stability values of the 25 assays. The first bar on the left contains the measured responses of stability to be compared with the ten remaining bars associated with ten simulations of the model (12). We observe a large similarity between the ten predictions and the observed stability. Table IV shows the mean confusion matrix of the stability predictions compared with the observations with a mean sensitivity: $S_e = 0.97$ and a mean specificity: $S_p = 0.95$, which corroborates the ability of the stability model to fit the observed data. Another global measure can be done : the percentage of correctness. In our case, we have 96.3% of correct answers over the 4000 replications.

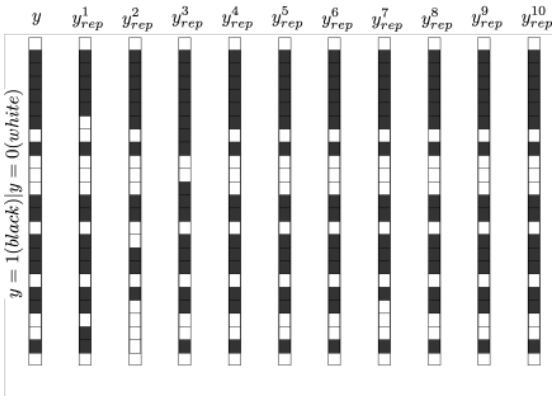

Fig. 3. Comparison of posterior predictions with the observations on stability. The first column on the left shows a vertical bar decomposed into 25 black/white segments associated with the stability values: black (stable) and white (unstable). The 10 bars on the right correspond to ten replications of posterior predictions.

TABLE IV

MEAN CONFUSION MATRIX ESTABLISHED OVER 4000 REPLICATES OF SIMULATION

	Observations	
Predictions	Stable	Unstable
Stable	14.55	0.38
Unstable	0.45	7.62

4) Design Space: once the stability model qualified, the subsequent design space is given by:

$$NOR_S = \{(\tilde{x}_2, \tilde{x}_4) \ ; \ \mathbb{P}(\tilde{Y}_s \text{ is stable} \mid \tilde{x}_2, \tilde{x}_4) \geq 0.9\} \tag{13}$$

$$PAR_S = \{(\tilde{x}_2, \tilde{x}_4) \ ; \ 0.7 \leq \mathbb{P}(\tilde{Y}_s \text{ is stable} \mid \tilde{x}_2, \tilde{x}_4) < 0.9\} \tag{14}$$

$$OOS_S = \{(\tilde{x}_2, \tilde{x}_4) \ ; \ \mathbb{P}(\tilde{Y}_s \text{ is stable} \mid \tilde{x}_2, \tilde{x}_4) < 0.7\} \tag{15}$$

The three associated regions of the design space can easily be represented in the plan (x_2;x_4) in Figure 4.

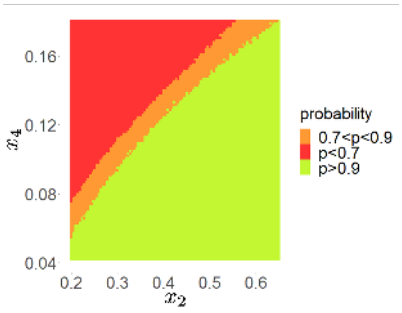

Fig. 4. Design Space of the LNP Stability. Region NOR in green has a stability probability greater than 90%. Region PAR (orange) has a stability probability between 70% and 90% while the last region: OOS in red has less then 70% to get LNP stability

B. Estimation Results for the siRNA Transfection Model

TABLE V
BF VALUES FOR THE EFFICIENCY RESPONSE (SAVAGE-DICKEY DENSITY RATIO)

Variable	BF
X_1	0.112
X_2	1.141
X_3	0.101
X_4	0.08

1) Model Selection: values of BF in Table V show that X_2 (PEG concentration) is the most critical factor impacting on the transfection efficiency. At the opposite, the LNP size (X_4) is the least influential factor. The two other factors: X_1 and X_3 (DOTAP and Lecithin proportions) do not appear as active factors but are kept for the estimation step.

2) Parameter Estimation: after the variable selection, the reduced structure of the transfection efficiency model (10) is composed of four parameters: $\beta = (\beta_0, \beta_1, \beta_2, \beta_3)'$ corresponding to the intercept coefficient and additive effects for X_1, X_2 and X_3 respectively on the transfection efficacy. The estimated values of the model parameters, provided by the MCMC technique, are given in Table VI. Figure 5 shows the posterior distributions of the logistic model parameters. Sign of β_2 indicates that the probability of efficiency is increasing when both X_2 (PEG proportion) is falling. The same remark can be made on X_3 (Lecithin proportion) on a smaller scale. On the other hand, the distribution of X_1 is centered on zero, synonym of a negligible effect compared to the two previous factors. Therefore, only X_2 and X_3 will be used to compute the transfection efficiency design space.

TABLE VI
ESTIMATED VALUES, STANDARD DEVIATIONS, AND MAIN QUANTILES FOR THE LOGISTIC MODEL PARAMETERS.

Parameter	Mean	SD	10%	50%	90%
b_0	1.7	2.1	-1.0	1.7	4.2
b_1	0.2	2.3	-2.7	0.2	3.2
b_2	-5.4	2.5	-8.6	-5.5	-2.2
b_3	-3.2	2.8	-6.6	-3.2	0.3

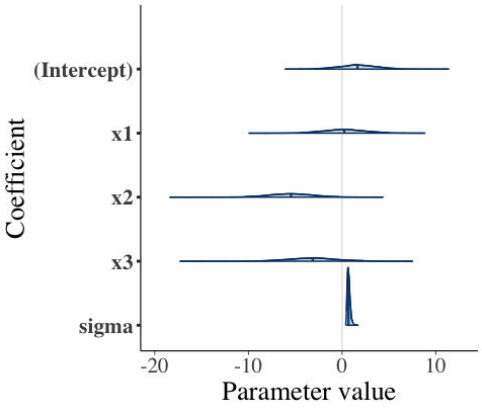

Fig. 5. Posterior distribution of the three parameters involved in the transfection efficiency logistic model

3) Model evaluation: the posterior predictive check was applied to the transfection model to assess its appropriateness to fit the data. Figure 6 presents four different ways to describe the dispersion of simulations (light blue) compared with the measurement (dark blue). In each plot, we observe a large similarity between the

predictions and the observed transfection efficiency. The *ppp-value* associated to the means (4th illustration) is equal to 0.505, very close to the targeted value: 0.5, which emphasizes the ability of the model to fit mean responses of the transfection efficiency. Nevertheless, PPC can be sometimes too optimistic and has to be corroborated by the Leave-One-Out Cross-Validation test.

The p_{LOO} value associated with the LOO test is equal to 4.9 (SE=2.0), close to the number of model parameters. Results of the Leave-One-Out Cross-Validation are shown in Figure 7. Only one out of 15 observations is not included in the posterior predictive distributions, which shows an acceptable accuracy of the model to describe the transfection efficiency response of the tested LNP.

4) Design Space: once the stability model qualified, the subsequent design space is given by:

$$NOR_E = \{(\tilde{x}_2, \tilde{x}_3) \ ; \ \mathbb{P}(\tilde{Y}_e \geq 30\% \mid \tilde{x}_2, \tilde{x}_3) \geq 0.9\} \tag{16}$$

$$PAR_E = \{(\tilde{x}_2, \tilde{x}_3) \ ; \ 0.7 \leq \mathbb{P}(\tilde{Y}_e \geq 30\% \mid \tilde{x}_2, \tilde{x}_3) < 0.9\} \tag{17}$$

$$OOS_E = \{(\tilde{x}_2, \tilde{x}_3) \ ; \ \mathbb{P}(\tilde{Y}_e \geq 30\% \mid \tilde{x}_2, \tilde{x}_3) < 0.7\} \tag{18}$$

The three associated regions of the design space can easily be represented in the (x_2;x_3) plan in Figure 8.

C. Final compromise

As emphasized by the two individual design spaces related to LNP stability and siRNA transfection efficiency, described in Figures 4 and 8 respectively, the second critical factor x_2 (PEG proportion) is involved in both design spaces and a compromise has to be determined. To that aim, we assume that the two CQA are independent from each other and the subsequent joint probability becomes:

$$\mathbb{P}(\tilde{Y}_s \text{ is stable} \,\&\, \tilde{Y}_e \text{ is efficient}) \tag{19}$$

$$= \mathbb{P}(\tilde{Y}_s \text{ is stable}) \times \mathbb{P}(\tilde{Y}_e \text{ is efficient}) \tag{20}$$

This formula allows us to estimate the global design spaces for x_2, x_3 and x_4 presented in Figure 9 in which the green area is the normal operating region. It shows there exists a very small NOR region in which combinations of values for the three critical factors could meet specifications on transfection efficiency and stability attributes.

IV. Discussion

Results of this study firstly emphasizes the practical relevance of a full Bayesian approach to implement the Quality-by-Design good practices in situations where only small experimental datasets are available. Such a situation is common and often dictated by limited budget and resources during the development phase, which generally leads developers to implement statistical strategies for the design of their experiments in order to minimize the number of tests. In this case, the Bayesian paradigm allowed us to account for prior knowledge gained through previous pilot assays. Over the last decade or so, a lot of contributions have made available computational tools in free software environments for statistical computing, such as the programming environments R and Python, to facilitate the implementation of Bayesian estimation methods. Results presented in this study also point out how the Bayesian framework is able to address risk assessment in a more extended scope and not only for parameter estimation as usually observed. The proposed Bayesian method for design space identification relies on five steps: design of experiments, variable selection, parameter estimation, model evaluation and design-space computation. Such a generic

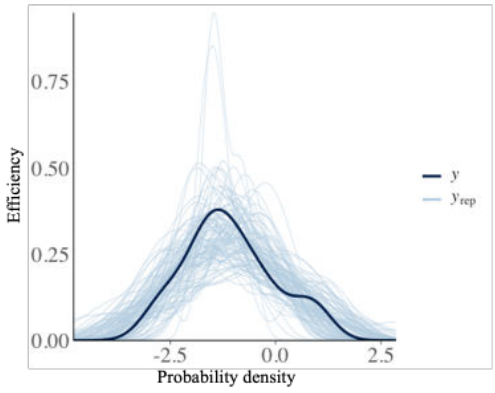

(a) Observed vs replicated transfection distributions

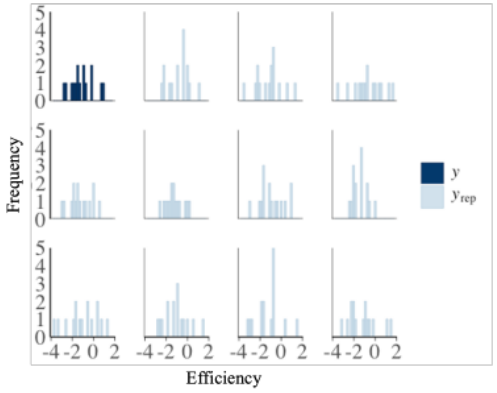

(b) Observed vs replicated data histogram

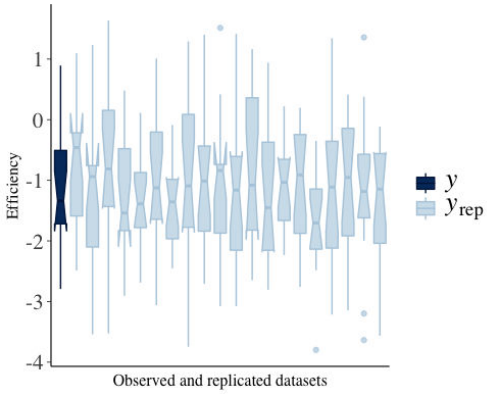

(c) Observed vs replicated data boxplots

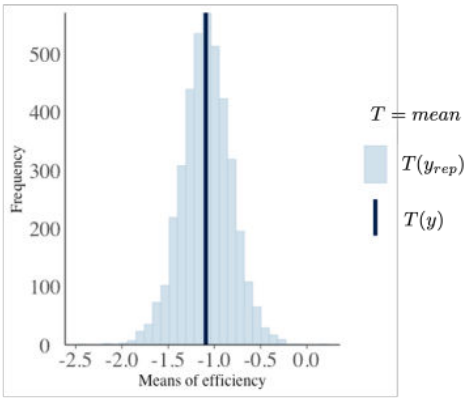

(d) Observed vs replicated average values of the transfection predictions

Fig. 6. Posterior predictive check of the transfection efficiency predictions. $y = \log\left(\frac{Y_{e,i}}{1-Y_{e,i}}\right)$ and y_{rep} denotes predicted values of y.

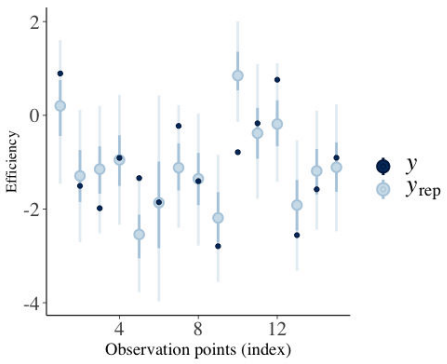

Fig. 7. Results of the Leave-One-Out Cross-Validation test. Observations are described by dark blue dots while posterior predictive distributions are plot in light blue.

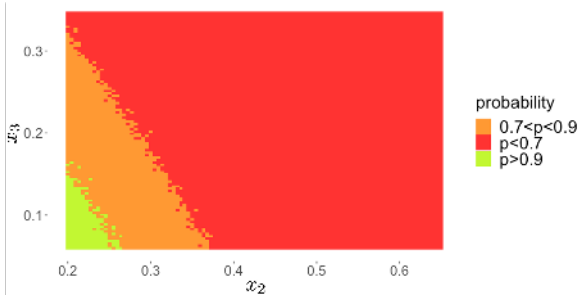

Fig. 8. Design Space of the siRNA transfection efficiency. Region NOR in green has a stability probability greater than 90%. Region PAR (orange) has a stability probability between 70% and 90% while the last region: OOS in red has less than 70% to get LNP stability. This design space was obtained with $x_1 = 0.683$.

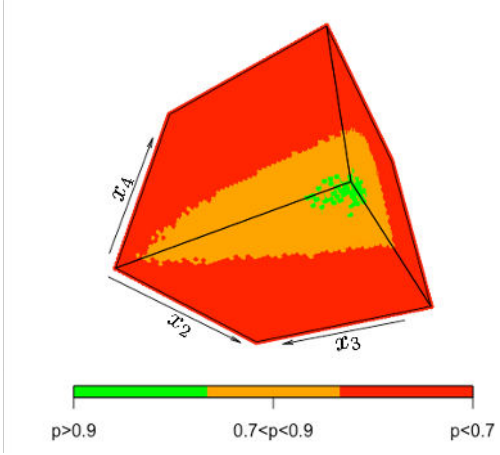

Fig. 9. Global Design Space integrating efficacy and stability specifications obtained for $x_1 = 0.683$. Region NOR in green has a stability probability greater than 90%. Region PAR (orange) has a stability probability between 70% and 90%, while the last region (OOS) in red has less than 70% to achieve LNP stability

methodology can be implemented in a large spectrum of applications even when response variables are not quantitative and when experimental data are missing, as emphasized in this study case.

Indeed, there are many categorical responses measured during physico-chemical characterization analysis such as functionality of surface chemistry, unchanged chemical identity, physical aggregation or resistance to sterilization process, etc. Therefore, it is quite important to get efficient method able to deal with this type of CQA.

The lack of data availability is also another generic issue caused by the elimination of experimental conditions leading to unstable or aggregated states that finally cannot be used to measure the other CQA. In this case, the statistical properties associated with the design of experiments are lost and can drastically increase the estimation uncertainty and therefore prevent us to draw any relevant conclusion.

Even when prior data coming from pilot studies are not available, we show that a weak information prior can in part compensate consequences of lost assays and provide relevant estimation results in practice. It has to be noted this estimation technique can be extrapolated to multi-value categorical response variables.

This Bayesian approach of QbD is currently being used in different projects involving molecules, nanoparticles and also medical devices, in two European projects: TBMED[2] and EXPERT[3]. In addition to the results highlighting the relevance of this approach, its implementation under the R statistical computing environment is quite simple.

In this study, one point was not addressed due to lack of budget. It concerns the validation of the Design Space and more precisely of the NOR region. This is a crucial point still underdeveloped in the literature that also deals with the design of experiments. What are the experimental points of the Design space for which new tests must be carried out to validate the delimitation of the NOR region? This question is all the more important when you consider that any point in this quality subspace is supposed to lead to equivalent drugs in terms of efficacy and safety. This operational flexibility must above all not lead to risks for the patient due to an error in the identification of the normal operating region.

V. Conclusions

This article has proposed a complete Bayesian approach of Quality-by-Design able to handle qualitative critical quality attributes and to compensate for data losses by introducing a weakly informative default prior. Our approach introduces new criteria to select critical process parameters such as the Bayes Factor but also to assess relevance of the model to fit the observed data such as the posterior predictive check and the leave-one-out cross correlation. The complete method and its

[2]https://tbmed.eu/

[3]https://www.expert-project.eu/

associated tools are described and their applicability is assessed through its application to the development of nanostructured lipid carriers dedicated to nucleic acid delivery. The two examined critical quality attributes: stability and siRNA transfection efficacy were described by two logistic models. The coefficients of both models were estimated by a Bayesian method implemented in the R computation environment. The proposed method also accounts for constraints on impossible values for the transfection response, which also contributes to improve the estimation accuracy. Among the four tested critical material attributes, only three have shown significant effects on the two CQAs: PEG and Lecithin proportions, and the LNP size, while the percentage of DOTAP did not produce any significant effect. Computed design spaces for the two CQAs demonstrated the existence of normal operating regions in which the probability to comply with the expected performance specifications is greater than 90%. Another advantage of the Bayesian paradigm is to handle the issue of multiple CQA specifications in a more natural way. A global design space was computed and enabled us to identify a compromise region of interest of ideal proportions.

APPENDIX A
MATERIAL CHARACTERIZATION

A. Materials

Suppocire NBTM was purchased from Gattefosse (Saint-Priest, France). Myrj 52TM, polyethylene glycol 40 stearate and Super Refined Soybean Oil were from CrodaUniqema (Chocques, France). Lipophilic cyanines, DiI and DiD, were purchased from Life technologies. Lipoid S75-3 (soybean lecithin) was from Lipoid (Germany). DOTAP was purchased from Avanti Polar Lipids (Alabaster, AL, USA). To perform gel retardation assays, GelRed was acquired from Interchim (Montluçon, France). For transfection assays, the commercial transfection reagent LipofectamineRNAiMax was from Life Technologies (Carlsbad, CA, USA) and other products were purchased from Qiagen (Hilden, Germany). Matrigel and cell recovery solution for 3D culture were provided by BD Biosciences (San Jose, CA, USA).

B. Cell culture conditions

Prostate carcinoma cells (PC3 cells) were obtained from ATCC (Ref. CRL-1435) and were routinely cultured in RPMI Glutamax culture media (Invitrogen, Ref. 61870-010) supplemented with 10% foetal calf serum (PAA, Ref. A15-101) and 1% penicillin/streptomycin (Invitrogen, Ref. 15140-122). Stable PC3 cell lines overexpressing green fluorescent protein (GFP) were also produced via transfection with pEGFPC1 plasmid (Clontech, CA, USA) using Lipofectamine®, according to provider recommendations.

HUVEC cells (primary human umbilical vein endothelial cell, ATCC® PCS-100-010™) were cultivated on fibronectin coated-6-well plates with EndoGRO complete medium provided by Millipore. Jurkat cells (immortalized line of human T lymphocyte cells (ATCC® TIB-152™) were cultivated with RPMI completed with 10% FBS. PC12 cells (cell line derived from a pheochromocytoma of the rat adrenal medulla, ATCC® CRL-1721™) were cultured on collagen IV coated wells with RPMI complemented with 10% heat inactivated horse serum, 5% FBS and 1% PS. PC12 cells were differentiated into a neuronal phenotype following 5 days incubation with 50 ng/mL mouse recombinant 2.5S NGF (nerve growth factor) in RPMI medium completed with 1% heat inactivated horse serum.

Three-dimensional culture was adapted from a protocol previously described by Dolega et al. [55]. Briefly, the 3D culture was grown in Matrigel (BD Biosciences, San Jose, CA) according to the top-coat protocol. Ma-

trigel was thawed overnight and poured into 4-well Labtec (160 μL of Matrigel, 500 μL of culture media) plates on ice. For polymerization, Matrigel was incubated for 30 min at 37°C. Cells were seeded in half the final volume and allowed to adhere for approximately 45 min (among 7.104 cells/well). The top coat layer containing 8% Matrigel was slowly poured over attached cells. The culture medium was changed every other day. Cells were cultured in a humidified atmosphere with 5% CO2 at 37°C. After 4-7 days, PC3-GFP cells were structured as spheroid forms and transfection assays were performed.

APPENDIX B
PHYSICO-CHEMICAL CHARACTERIZATION OF CNLC

This study case was focused on a subclass of solid lipid nanoparticles, cationic nanosized lipid carriers (cNLCs), into two states: as one entity or with modified siRNA as a nucleic acid delivery system. These nanoparticles present a high colloidal stability and excellent safety profile.

A. Formulation of cNLCs and siRNA nanocomplexes

siGFP-22 (Qiagen) is used to down-regulate GFP expression. Cationic nanostructured lipid carriers (cNLCs) were obtained by emulsion templating through ultrasonication according to a process previously described by Delmas *et al.*[39]. Both aqueous and lipid phases contained a blend of solid (Suppocire NCTM) and liquid (Super refined Soybean oil) glycerides with phospholipids (Lipoid S75-3^{TM}) and DOTAP, while the aqueous phase was composed of PEG surfactant (Myrj 52^{TM}) dissolved in 154 mM NaCl aqueous buffer. After homogenization at high temperature, both phases were crudely mixed. Sonication cycles were then performed during a 10mn period (VCX750 Ultrasonic processor, 3mm probe, Sonics, France; sonication power 23%). Non-encapsulated components were separated from the nanoparticle dispersion by gentle dialysis overnight in 154 mM NaCl against 1,000 times their volume (MWCO: 12,000 Da, ZelluTrans) with the dialysate changed twice during purification. Nanoparticle dispersions were filtered through 0.22 μm cellulosic membrane (Millipore) before use.

cNLC-siRNA nanocomplexes were constituted through electrostatic interactions within a variety of particle amine to siRNA phosphate ratios (N/P) settled according to the experimental assembly. In order do to so, the desired amount of siRNA, fixed at 20 μM siRNA (Qiagen), was incubated at room temperature with its corresponding amount of cNLC for 20 minutes to allow for spontaneous nanocomplex formation. The newly-formed nanocomplexes were then diluted in the buffer according to the desired final siRNA concentration. Lipofectamine-siRNA nanocomplexes were produced in a similar manner after considering different concentrations with the specific lipofectamine:siRNA ratio recommended by the manufacturer's instructions.

B. Size and zeta potential of both cNLC and siRNA nanocomplex

The hydrodynamic diameter and zeta potential of the cNLCs and cNLC-siRNA nanocomplexes were measured with a Zeta SizerNano (Malvern Instrument, NanoZS, UK) in 0.15mM NaCl using Zeta Sizer Nano cells (Malvern Instrument). The samples were equilibrated before measurement at 25°C for 2 minutes. cNLC measurements were made immediately after formulation. Average hydrodynamic diameter and polydispersity were extracted from cumulative analysis of the autocorrelation function on an intensity basis. Each measurement was performed in triplicate.

The hydrodynamic diameters were: 42.71 +/- 2.09 nm and 72.94 +/- 0.53 nm for cNLCa and cNLCb, respectively, and their polydispersity index were both lower than 0.2, indicating a monodisperse population. Moreover, a high cationic charge, greater than 20mV, was observed for both particles in 0.15mM NaCl buffer. As a matter of fact, a global positive charge is required in order to promote electrostatic bonds with anionic nucleic acid (RNA) and thus was achieved via the use of high DOTAP molar concentration in the cNLCa and cNLCb composition. Furthermore, both cNLCs displayed a high level of stability for up to 23 weeks in term of hydrodynamic diameter and zeta potential. Finally, with variation in their N/P ratio, cNLC-siRNA nanocomplexes formed compact structures ranging from 45-65 nm in size at all N/P ratios as well as low levels of polydispersity. All nanocomplexes exhibited a cationic surface charge displaying increase in their zeta potentials with the corresponding N/P ratio.

APPENDIX C
CNLC-SIRNA MEDIATED GFP INHIBITION IN 2D CULTURE

PC3-GFP cells were seeded in 12-well plates 24 hours prior to experiments at a density of $2.5 * 10^4$cells per well in growth medium. Prior to adding the cNLC-siRNA complexes, the cells were washed and briefly incubated with 300 μL/well of DMEM, 6.8% FBS at 37°C and 5% CO2. Subsequently, 200 μL of cNLC-siRNA nanocomplexes, typically containing 0.13 μg (20 nM) siRNA, were added to each well and cells were grown for a further 72 hours. The nanocomplexes' functional inhibition was compared to two different condition controls : first of all a transfection with nanoparticle complexed to scrambled siRNA (siAllstar, Qiagen), with no known target, and then with non-transfected cells. Following transfection, cells were analyzed by flow cytometry (FACS LSRII, Becton Dickinson, France). Finally, a comparison with a variety of commercially available transfection reagents was performed following the same protocol and in accordance with manufacturer's instructions.

GFP expression inhibition was also assessed at a protein level through the use of Western-Blot analysis. In order to do so, Transfected PC3-GFP cells were washed twice then added to RIPA lysis buffer containing complete protease inhibitor cocktail (Roche) and incubated for 10 min at 4°C. The lysates were centrifuged at 14000G for 10 min at 4°C and protein concentration was assessed using a BCA assay (Pierce). A 10 μg protein sample was resuspended in the appropriate volume of 10% SDS-containing Laemmli buffer and reducing agent (DTT) and then boiled for 5 min at 100°C. The samples were subsequently analyzed on a 4-12% gradient SDS-polyacrylamide gel electrophoresis (nuPAGE, Invitrogen). The proteins were then transferred onto a nitrocellulose membrane (Amersham, UK), blocked with nonfat dry milk in TBS 0.05% Tween 20 buffer and labeled mouse anti-GFP and anti α-tubulin antibodies, respectively, (Abcam, Cambridge, UK) at 1:5000 dilution overnight at 4°C. Anti-mouse IgG (Jackson Immunoresearch, PA, USA) was used at 1:5000 dilution to detect the GFP and α-tubulin following 1 hour incubation. Quantification of the data was performed using ImageJ software (n=3). The relative intensity was calculated by dividing the absolute intensity of each sample band by the absolute intensity of the standard (loading control).

When compared to the commercial agent Lipofectamine, cNLCa and cNLCb charged with 20 nM siRNA presented comparable down-regulation efficiency in terms of fluorescence inhibition (N/P =12/1) with GFP-cells. In the same way, siControl transfection with Lipofectamine was observed to stimulate GFP expres-

sion in contrast to transfection with cNLCs. However, with untreated cells, GFP inhibition was found to have significantly decreased with Lipofectamine RNAimax and cNLCa, yet remained unchanged with cNLCs. These findings were also observed at a protein level. Infact, according to Western-Blot results, the down-regulation efficiency after 48hours of transfection of 20 nM siGFP was less pronounced for cNLCb than cNLCa. The inhibition caused by cNLCa was actually higher than siGFP transfection with Lipofectamine RNAimax (seen as control). Therefore, the comparison with a variety of commercially available transfection reagents highlighted the high efficiency of cNLCa. Finally, the down-regulation efficiency of both cNLCs exhibited no significant changes during longer incubation experiments at room temperature, demonstrating the high stability of the nanocomplexes over time.

ACKNOWLEDGMENT

TBMED has received funding from the European Union's Horizon 2020 research and innovation programme under Grant Agreement no. 814439. EXPERT has received funding from the European Union's Horizon 2020 research and innovation programme under Grant Agreement no. 825828. The authors are solely responsible for its content, this paper does not represent the opinion of the European Commission and the Commission is not responsible for any use that might be made of data appearing therein.

REFERENCES

[1] ICH Expert Working Group, *Pharmaceutical Development Q8(R2)*, International Conference on Harmonisation, August 2009.

[2] D. van de Berg, Z. Kis, C. F. Behmer, K. Samnuan, A. K. Blakney, C. Kontoravdi, R. Shattock, and N. Shah, "Quality by design modelling to support rapid rna vaccine production against emerging infectious diseases," *npj Vaccines*, vol. 6, no. 1, pp. 1–10, 2021.

[3] A. S. Rathore and H. Winkle, "Quality by design for biopharmaceuticals," *Nature biotechnology*, vol. 27, no. 1, pp. 26–34, 2009.

[4] T. Bastogne, "Quality-by-design of nanopharmaceuticals – A state of the art," *Nanomedicine: Nanotechnology, Biology and Medicine*, vol. 13, no. 7, pp. 2151–2157, 2017.

[5] J. J. Peterson and M. Yahyah, "A bayesian design space approach to robustness and system suitability for pharmaceutical assays and other processes," *Statistics in Biopharmaceutical Research*, vol. 1, no. 4, pp. 441–449, 2009. [Online]. Available: https://doi.org/10.1198/sbr.2009.0037

[6] G. W. Stockdale and A. Cheng, "Finding design space and a reliable operating region using a multivariate bayesian approach with experimental design," *Quality Technology & Quantitative Management*, vol. 6, no. 4, pp. 391–408, 2009. [Online]. Available: https://doi.org/10.1080/16843703.2009.11673206

[7] J. J. Peterson and K. Lief, "The ich q8 definition of design space: A comparison of the overlapping means and the bayesian predictive approaches," *Statistics in Biopharmaceutical Research*, vol. 2, no. 2, pp. 249–259, 2010. [Online]. Available: https://doi.org/10.1198/sbr.2009.08065

[8] P. Lebrun, B. Boulanger, B. Debrus, P. Lambert, and P. Hubert, "A bayesian design space for analytical methods based on multivariate models and predictions," *Journal of Biopharmaceutical Statistics*, vol. 23, no. 6, pp. 1330–1351, 2013, pMID: 24138435. [Online]. Available: https://doi.org/10.1080/10543406.2013.834922

[9] Committee for Human Medicinal Products, "ICH guideline Q8 (R2) on pharmaceutical development," European Medicine Agency, Tech. Rep. Step 5, June 22 2017.

[10] P. Borman, C. Campa, G. Delpierre, E. Hook, P. Jackson, W. Kelley, M. Protz, and O. Vandeputte, "Selection of analytical technology and development of analytical procedures using the analytical target profile," *Analytical Chemistry*, 2021.

[11] A. Gelman, J. B. Carlin, H. S. Stern, D. B. Dunson, A. Vehtari, and D. B. Rubin, *Bayesian data analysis*, 2010, vol. 1, no. 5.

[12] E. Lesaffre, G. Baio, and B. Boulanger, *Bayesian Methods in Pharmaceutical Research*. CRC Press, 2020.

[13] FDA, "Guidance for the use of bayesian statistics in medical device clinical trials," Guidance for Industry and FDA Staff. Center for Devices and Radiological Health, Division of Biostatistics, Office of Surveillance and Biometrics, Tech. Rep., February 2010.

[14] ——, "Meta-analyses of randomized controlled clinical trials to evaluate the safety of human drugs or biological products guidance for industry," U.S. Department of Health and Human Services Food and Drug Administration. Center for Drug Evaluation and Research (CDER) Center for Biologics Evaluation and Research (CBER), Tech. Rep., November 2018.

[15] ——, "Biomarker qualification: Evidentiary framework - guidance for industry and fda staff," U.S. Department of Health and Human Services Food and Drug Administration, Drug Development Tools, Tech. Rep., December 2018.

[16] A. S. Zidan, O. A. Sammour, M. A. Hammad, N. A. Megrab, M. J. Habib, and M. A. Khan, "Quality by design: Understanding the formulation variables of a cyclosporine a self-nanoemulsified drug delivery systems by box–behnken design and desirability function," *International journal of pharmaceutics*, vol. 332, no. 1, pp. 55–63, 2007.

[17] M. Kakran, N. Sahoo, L. Li, Z. Judeh, Y. Wang, K. Chong, and L. Loh, "Fabrication of drug nanoparticles by evaporative precipitation of nanosuspension," *International Journal of Pharmaceutics*, vol. 383, no. 1–2, pp. 285 – 292, 2010.

[18] Y. B. Pawar, H. Purohit, G. R. Valicherla, B. Munjal, S. V. Lale, S. B. Patel, and A. K. Bansal, "Novel lipid based oral formulation of curcumin: development and optimization by design of experiments approach," *International journal of pharmaceutics*, vol. 436, no. 1, pp. 617–623, 2012.

[19] S. Martins, I. Tho, E. Souto, D. Ferreira, and M. Brandl, "Multivariate design for the evaluation of lipid and surfactant composition effect for optimisation of lipid nanoparticles," *European Journal of Pharmaceutical Sciences*, vol. 45, no. 5, pp. 613–623, 2012.

[20] S.-J. Park, G.-H. Choo, S.-J. Hwang, and M.-S. Kim, "Quality by design: screening of critical variables and formulation optimization of Eudragit E nanoparticles containing dutasteride," *Archives of Pharmacal Research*, vol. 36, no. 5, pp. 593–601, 2013.

[21] K. Raza, B. Singh, P. Singal, S. Wadhwa, and O. P. Katare, "Systematically optimized biocompatible isotretinoin-loaded solid lipid nanoparticles (slns) for topical treatment of acne," *Colloids and Surfaces B: Biointerfaces*, vol. 105, pp. 67–74, 2013.

[22] S. Kumar, R. Gokhale, and D. J. Burgess, "Quality by design approach to spray drying processing of crystalline nanosuspensions," *International Journal of Pharmaceutics*, vol. 464, no. 1–2, pp. 234 – 242, 2014.

[23] S. Beg, G. Sharma, K. Thanki, S. Jain, O. P. Katare, and B. Singh, "Positively charged self-nanoemulsifying oily formulations of olmesartan medoxomil: Systematic development, in vitro, ex vivo and in vivo evaluation," *International Journal of Pharmaceutics*, vol. 493, no. 1-2, pp. 466–482, SEP 30 2015.

[24] F. Rose, J. E. Wern, P. T. Ingvarsson, M. van de Weert, P. Andersen, F. Follmann, and C. Foged, "Engineering of a novel adjuvant based on lipid-polymer hybrid nanoparticles: A quality-by-design approach," *Journal of Controlled Release*, vol. 210, pp. 48–57, 2015.

[25] L. Mandpe and V. Pokharkar, "Quality by design approach to understand the process of optimization of iloperidone nanostructured lipid carriers for oral bioavailability enhancement," *Pharmaceutical development and technology*, vol. 20, no. 3, pp. 320–329, 2015.

[26] V. Nekkanti, A. Marwah, and R. Pillai, "Media milling process optimization for manufacture of drug nanoparticles using design of experiments (doe)," *Drug development and industrial pharmacy*, vol. 41, no. 1, pp. 124–130, 2015.

[27] A. E. Shirsat and S. S. Chitlange, "Application of quality by design approach to optimize process and formulation parameters of rizatriptan loaded chitosan nanoparticles," *Journal of Advanced Pharmaceutical Technology & Research*, vol. 6, no. 3, pp. 88–96, Jul-Sep 2015.

[28] P. Lebrun, B. Govaerts, B. Debrus, A. Ceccato, G. Caliaro, P. Hubert, and B. Boulanger, "Development of a new predictive modelling technique to find with confidence equivalence zone and design space of chromatographic analytical methods," *Chemometrics and Intelligent Laboratory Systems*, vol. 91, no. 1, pp. 4 – 16, 2008. [Online]. Available: http://www.sciencedirect.com/science/article/pii/S0169743907001165

[29] E. Rozet, P. Lebrun, P. Hubert, B. Debrus, and B. Boulanger, "Design spaces for analytical methods," *TrAC Trends in Analytical Chemistry*, vol. 42, no. 0, pp. 157 – 167, 2013. [Online]. Available: http://www.sciencedirect.com/science/article/pii/S0165993612002786

[30] M. G. Blum, "Regression approaches for approximate bayesian computation," *arXiv preprint arXiv:1707.01254*, 2017.

[31] K. Csilléry, M. G. Blum, O. E. Gaggiotti, and O. François, "Approximate bayesian computation (abc) in practice," *Trends in ecology & evolution*, vol. 25, no. 7, pp. 410–418, 2010.

[32] G. E. P. Box and N. R. Draper, *Empirical Model-Building and Response Surfaces*. Wiley, 1987.

[33] G. A. Lewis, D. Mathieu, and R. Phan-Tan-Luu, *Pharmaceutical Experimental Design*. Marcel Dekker, 2005.

[34] D. W. Heck, "A caveat on the savage–dickey density ratio: The case of computing bayes factors for regression parameters," *British Journal of Mathematical and Statistical Psychology*, vol. 72, no. 2, pp. 316–333, 2019.

[35] A. Gelman, A. Jakulin, M. G. Pittau, and Y. S. Su, "A weakly informative default prior distribution for logistic and other regression models," *Annals of Applied Statistics*, vol. 2, no. 4, pp. 1360–1383, 2008.

[36] D. W. Heck, "A caveat on the savage–dickey density ratio: the case of computing bayes factors for regression parameters," *British Journal of Mathematical and Statistical Psychology*, vol. 72, no. 2, pp. 316–333, 2019.

[37] A. Gelman, "Two simple examples for understanding posterior p-values whose distributions are far from uniform," *Electronic Journal of Statistics*, vol. 7, pp. 2595–2602, 2013.

[38] A. Vehtari, J. Gabry, Y. Yao, and A. Gelman, "loo: Efficient

leave-one-out cross-validation and waic for bayesian models," *R package version*, vol. 2, no. 0, p. 1003, 2018.

[39] T. Delmas, A.-C. Couffin, P. A. Bayle, F. De Crecy, E. Neumann, F. Vinet, M. Bardet, J. Bibette, and I. Texier, "Preparation and characterization of highly stable lipid nanoparticles with amorphous core of tuneable viscosity," *Journal of colloid and interface science*, vol. 360, no. 2, pp. 471–481, 2011.